Chapter L

A Sequence of Very Shallow Earthquakes in the Rock Valley Fault Zone, Southern Nevada Test Site

By Kenneth D. Smith,[1] G. Shields,[1] *and* James N. Brune[1]

Contents

Figures

Tables

[For table of abbreviations and conversions, click here]

[1]University of Nevada-Reno Seismological Laboratory, Reno, Nev.

Abstract

A sequence of unusually shallow (depth < 3 kilometers) earthquakes occurred in the southern Nevada Test Site in mid-1993 within the Rock Valley fault zone, a system that has shown Holocene activity. The largest earthquake of the sequence was an M_L 3.7 event on May 31, 1993. This earthquake activity included 140 events that triggered the local short-period network and approximately 500 additional smaller earthquakes that were recorded on a near-source three-component portable instrument over a 5-month period. The shallow depth of the 1993 sequence is demonstrated by extremely short *S* minus *P* times measured from clear body-wave arrivals on the near-source seismograph for nearly the entire sequence. The focal mechanisms of the larger events show left-lateral strike-slip motion on a steeply dipping northeast-striking fault segment in Rock Valley. Until the June 1992 Little Skull Mountain earthquake, only one M 3+ event had been reported in the Rock Valley fault zone since comprehensive regional seismic monitoring began in 1978. Since 1992 and through mid-1998, a number of M 3.5+ events have been recorded in Rock Valley, suggesting a relationship between the Little Skull Mountain event and the Rock Valley fault zone.

Introduction

A remarkable series of shallow earthquakes (hypocentral depth < 3 km) occurred in the Rock Valley fault zone (RVFZ) on the Nevada Test Site (NTS) in mid-1993. The shallow depth of the sequence is demonstrated by the extremely short *S* minus *P* times observed from clear horizontal-component *S*-wave arrivals on a near-source three-component seismograph. The largest earthquake of the sequence was an M_L 3.7 event on May 31, 1993. The short-period focal mechanisms of the larger events of the sequence show left-lateral strike-slip motion on steeply dipping northeast-striking structures. This activity included 140 events that triggered the Southern Great Basin Seismic Network (SGBSN) and an additional 500 smaller earthquakes recorded on a near-source portable instrument. Until the 1992 Little Skull Mountain earthquake, only one M 3+ earthquake had been reported in Rock Valley since comprehensive regional seismic monitoring began in 1978. Since the Little Skull Mountain (LSM) earthquake, and through mid-1998, four M 3.5+ earthquakes have been recorded in the RVFZ.

Tectonic earthquakes at such shallow depths have rarely been confirmed in California (Fletcher and others, 1987; Frankel and others, 1986) and Nevada. A depth of 5 km is typically the upper limit of the "seismogenic zone," the depth range where the lithostatic pressure from the weight of overlying rock is high enough, and the coefficient of friction is high enough, to stress the rocks to the level required for stick-slip faulting behavior. Because the Rock Valley earthquakes are near the upper limit of the seismogenic zone, they are of fundamental interest for earthquake mechanics. At such low lithostatic stress values, the magnitude and orientation of the local tectonic stresses may play a particularly important role in generating shallow earthquakes. The ground motion generated from shallow earthquakes may be important for design considerations for a potential radioactive-waste repository and support facilities at Yucca Mountain.

The 1993 Rock Valley earthquake sequence was confined to the RVFZ, an east-northeast-striking fault system showing Holocene displacement that spans most of the southern NTS (fig. 1). A detailed study of the RVFZ describing its segmentation geometry and its role in the tectonics of the south-central NTS is presented by O'Leary (this volume). The RVFZ establishes a physiographic and tectonic boundary between a cover of mid-Tertiary volcanic tuffs to the north and early Paleozoic rocks that make up the Specter and Spotted Ranges to the south. It is one of several mapped fault systems in the central and southern NTS that strike northeasterly, although it trends more easterly than the other systems (Carr, 1984). In addition to the RVFZ, these are the Mine Mountain, Wahmonie, and Cane Spring fault zones (fig. 1).

Shallow earthquakes previously observed on the NTS have been directly associated with underground nuclear testing. Hamilton and others (1971) reported on an extended sequence of shallow earthquakes triggered by a series of megaton tests that were recorded on a temporary seismic array in the Pahute Mesa area (fig. 1) in the late 1960's and early

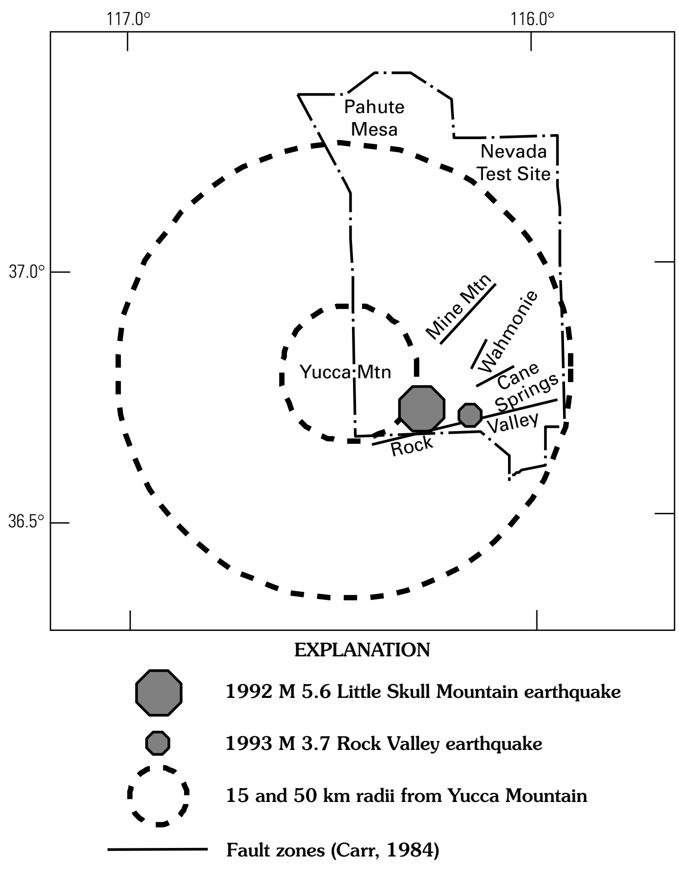

Figure 1. Faults of south-central Nevada Test Site. Shown are location of the 1992 Little Skull Mountain earthquake and main event of the 1993 Rock Valley sequence.

1970. These authors determined the depths for most of these earthquakes to be similar to that of the 1993 Rock Valley sequence (< 5 km). This Pahute Mesa activity included several thousand earthquakes, some reported to be as large as M 3.5. Hamilton and others (1971) determined the fault-plane solutions for a number of these events and associated the alignment of the seismicity with northeast-striking faults in the Pahute Mesa area.

Figure 2 shows earthquakes of the SGBSN catalog from 1978 through the M 5.6 June 29, 1992, LSM earthquake. Shown in figure 2 are the two M 3 earthquakes in the catalog for this area. The M 3+ earthquake near the epicenter of the Little Skull Mountain earthquake was an immediate foreshock to that event; the other M 3+ event took place in mid-1982. An M 3+ earthquake was also reported in the RVFZ in 1970, prior to the installation of the short-period regional SGBSN. Also, three earthquakes (M 3+) recorded on seismographs in California in 1948 may also have taken place in the RVFZ. (See von Seggern and Brune, this volume.) These 1948 events show waveforms similar to recent Rock Valley and Little Skull Mountain aftershock records at the same California stations that have been operating since the 1940's.

The 1992 LSM earthquake (Harmsen, 1994; Meremonte and others, 1995; Smith and others, this volume) was the largest earthquake in the southern Basin and Range since the 1966 M_L 5.7–6.1, Caliente, Nev., event some 100 km to the northeast (Rogers and others, 1991). The May 17, 1993, M 6 Eureka Valley, Calif., earthquake has since become the most recent moderate-sized southern Great Basin earthquake. Although the fault plane of the LSM earthquake projects to the surface in southern Jackass Flat and north of the RVFZ, earthquake activity in the central and south-central NTS region during the LSM aftershock period was distributed in a wide zone coincident with previous background seismicity. With the exception of those areas associated with underground nuclear tests, the western RVFZ has been one of the most seismically active areas on the NTS since comprehensive seismic monitoring began in 1978. Also, as evidenced by the 1948 earthquakes, this has mostly likely been an area of continued seismic activity.

This report is a preliminary analysis of the 1993 RVFZ seismicity using SGBSN data and recordings from two portable seismic instruments. In addition to the 1993 Rock Valley sequence, we also discuss other seismicity in and around the RVFZ since the LSM earthquake. This has included several M 3.5+ events and a relatively shallow cluster of seismicity in 1993 (fig. 3) east of the NTS. Shields and others (1995) have determined the source parameters of a number of the larger events of the 1993 sequence from analysis of the portable instrument waveform data.

Acknowledgments

We wish to thank Martha K. Savage and John Schneider for their reviews and helpful comments.

Seismic Data

Signals from the short-period stations of the SGBSN are transmitted by microwave to the University of Nevada-Reno Seismological Laboratory where they are digitized at 100 samples per second and passed through the CUSP processing system (Peppin and Nicks, 1992). The magnitude detection threshold varies throughout the SGBSN but is considered to be complete to approximately M 1.5 (Gomberg, 1991). On May 16, 1993, two M 3 events were located at shallow depths in the RVFZ in the sequence area. This motivated the deployment of two portable seismic recorders. One of these instruments was placed in the near-source region (station RTPP) and the other was put west of Frenchman Flat near Hampel Hill (station RHAM), 8 km to the northeast (fig. 4). This second instrument was deployed east of the activity to supplement network azimuthal coverage, and both of these recorders were configured with broadband three-component velocity sensors. The near-source station (RTPP) recorded more than 600 events from the source region from May through September 1993; 140 of these were large enough to trigger the SGBSN.

Phase arrival times and first motions determined from portable data were merged with SGBSN arrival times. Including near-source *P*- and *S*-wave arrival times significantly improves the location quality, and horizontal component *S*-waves are critical for resolving hypocentral depths. Near-source *S*-wave arrivals can place constraints on earthquake depths even though some question about the actual velocity structure may arise. A rule-of-thumb for acquiring accurate depth resolution is that a seismic station should be situated within one hypocentral depth. Station RTPP clearly meets this criterion. Gomberg (1990) discussed the role of *S*-waves in constraining earthquake locations using SGBSN records.

In order to determine a more accurate set of earthquake locations, we have applied an average station residual method. We initially located the 12 largest events recorded on both portable instruments and the network with a common set of the 28 closest seismic stations, using the one-dimensional velocity model of Hoffman and Mooney (1984). From the initial set of locations, the average travel-time residual at each station was applied in a subsequent location of the 140 earthquakes that triggered the SGBSN and these 28 stations. This technique accounts for misfits between the true three-dimensional velocity structure with respect to the one-dimensional velocity model and also accounts for local site effects at each recording station. It is most effective for determining relative locations when applied to groups of earthquakes in a limited source region, which is the case for the Rock Valley sequence. All recording stations are assumed to be on a datum elevation and therefore depths are reported relative to the mean surface elevation. The technique accounts for the elevation above the datum in an approximate way as a site correction. Figure 4*A* shows the relocated epicenters for the May through November 1993 time period. Also shown (fig. 4*B*) are the *P*-wave first-motion focal mechanisms for 10 of these earthquakes.

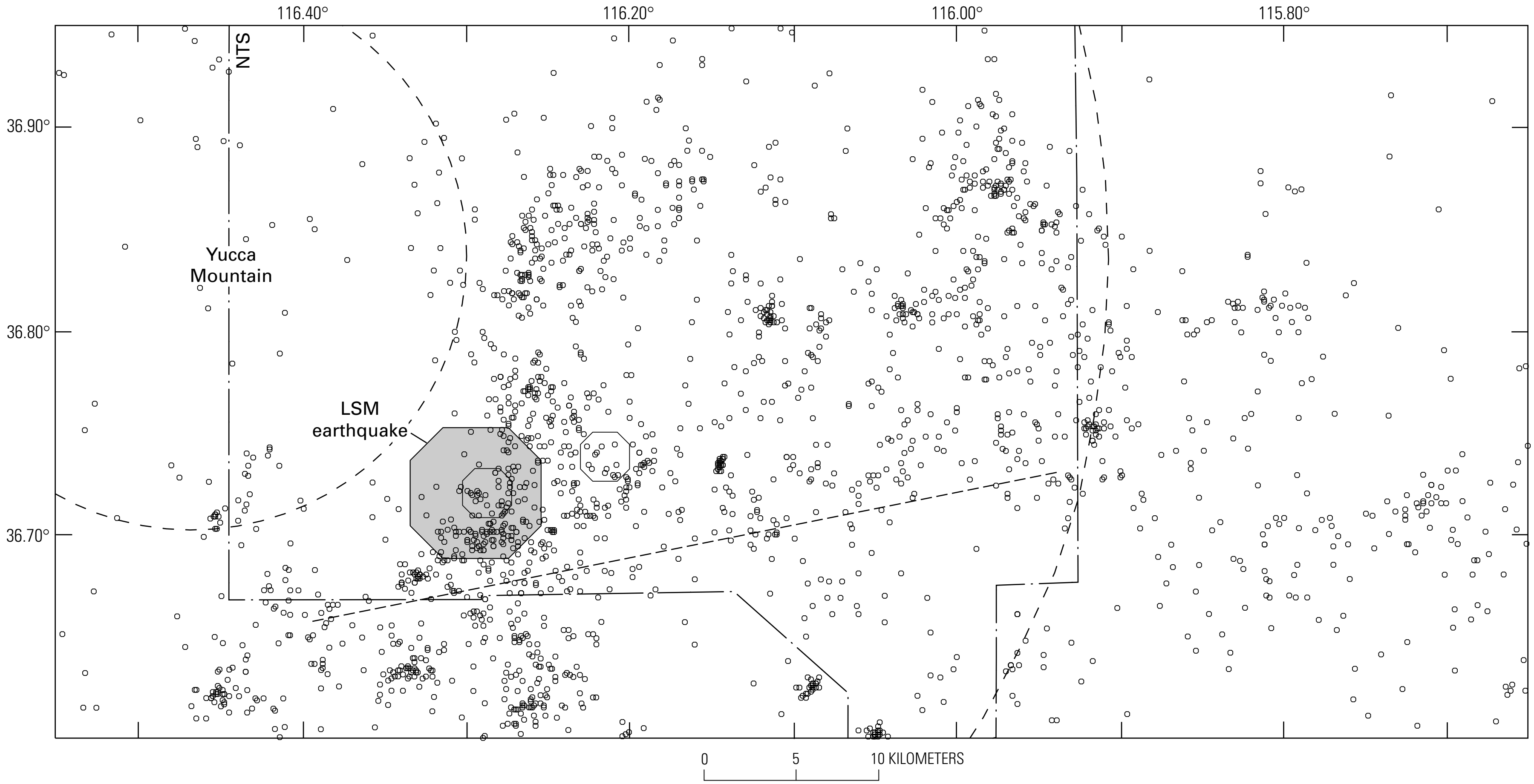

Figure 2. Earthquake activity in southern Nevada Test Site from 1978 through the June 29, 1992, Little Skull Mountain earthquake. Location of Little Skull Mountain event is shown by large shaded symbol; two mid-sized symbols represent M 3+ events recorded during this time period. Dashed arcs, 15 and 50 km radii from Yucca Mountain. Dashed straight line, general trend of RVFZ.

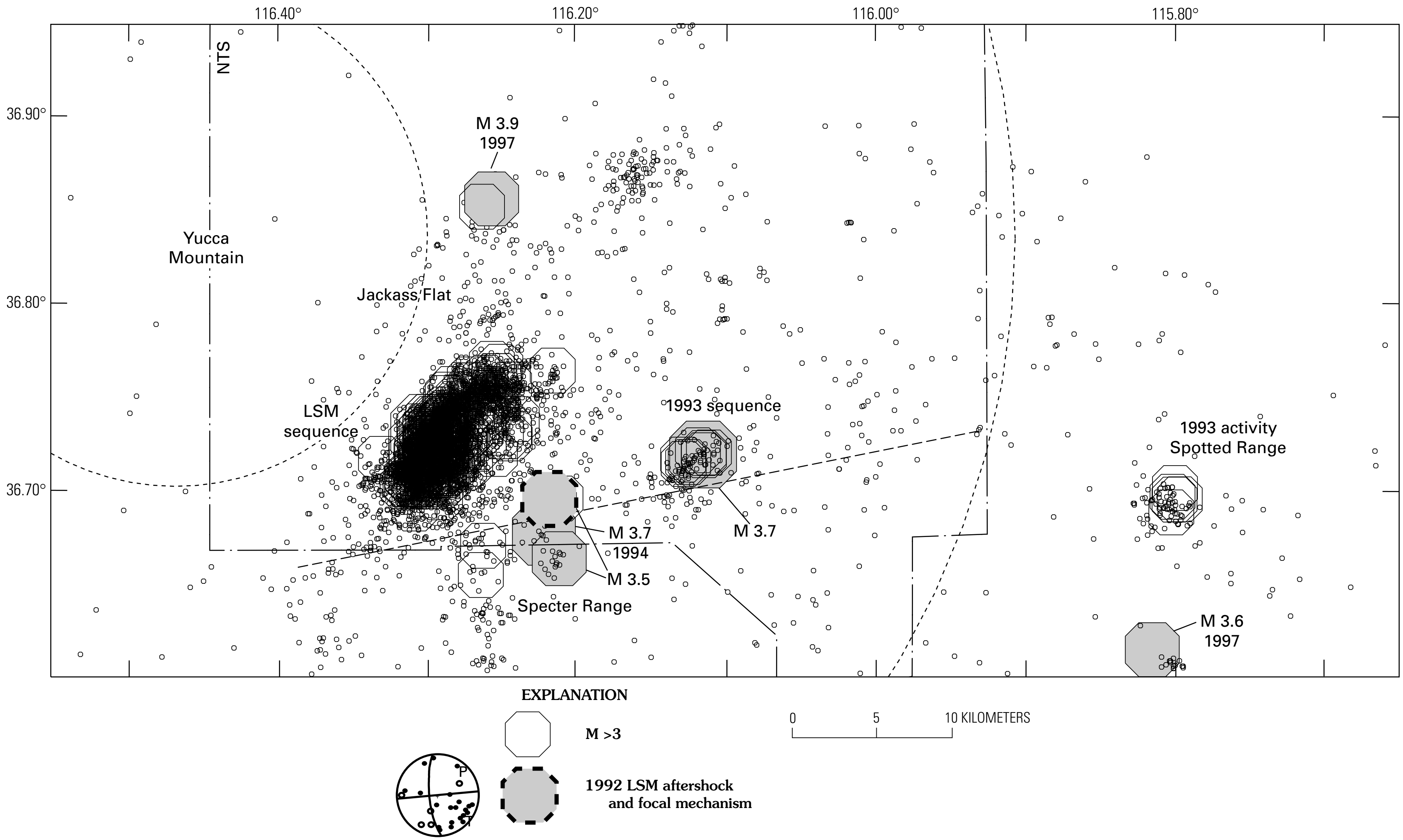

Figure 3. Earthquakes in southern Nevada Test Site from the June 29, 1992, Little Skull Mountain earthquake through September 1995. Dashed straight line, general trend of RVFZ. Shaded octagons indicate M ≥ 3.5 events.

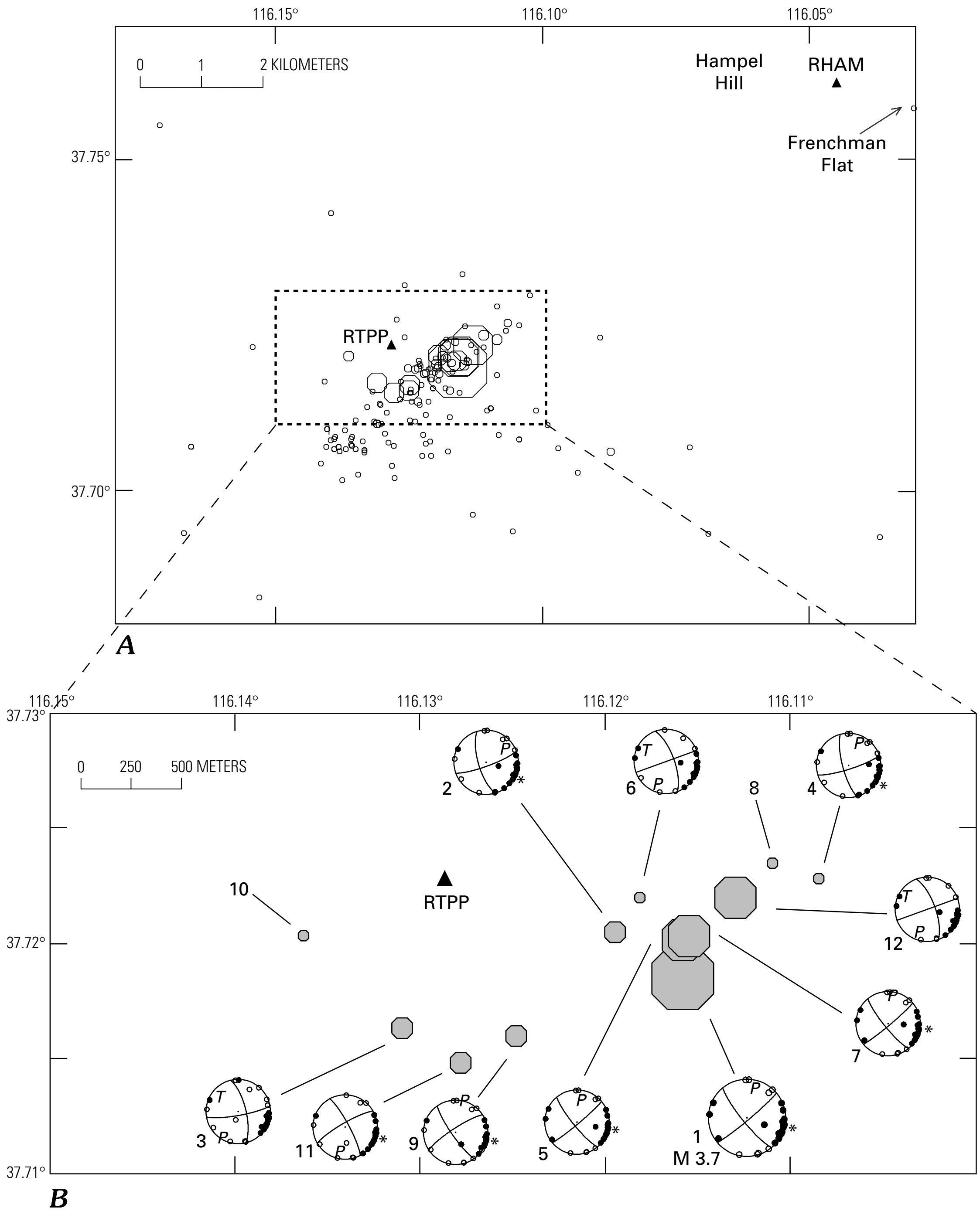

Figure 4. Earthquakes of 1993 Rock Valley sequence from May through September 1993. *A*, Relocation of 140 earthquakes of the sequence. *B*, Expanded view of part of *A*, showing *P*-wave first-motion focal mechanisms for 10 of these earthquakes. T-axis is labeled "*T*," except where obscured, in which case an asterisk (*) is placed outside the circle.

1993 Rock Valley Sequence

Main Event

The largest event of the 1993 Rock Valley sequence occurred at 15:20 UT (Universal Time) on May 30, fifteen days following deployment of the portable instruments, and approximately 12 km east of the LSM aftershock zone (fig. 3). This particular area was not active during the LSM aftershock sequence, although there was activity within the RVFZ during the LSM sequence (fig. 3). The relocated hypocenter for the main event is listed in table 1 (Event #1). Savage and Anderson (1995) and Shields and others (1995) have reported an M_L of 3.7 and an M_W of 3.7 from analyses of regional records, respectively. The equal-area lower-hemisphere short-period focal mechanism is shown in figure 4*B* (Event #1). The preferred fault plane is selected based on the alignment of seismicity and

Table 1. Event summary.

[EV#, event number; origin time, year-month-day-hour-minute-second; Z, event depth (km) after relocation using layered velocity model; Z*, depth fixed by *S* minus *P* time at station RTPP and assuming a 3.0 km/s *P*-wave velocity; M_D, network duration magnitude; M_W, moment-magnitudes from Shields and others (1995); gap, location gap in degrees; rms, root mean square *P*-wave residual in seconds; *S-P*, *S* minus *P* time (seconds) at station RTPP]

EV#	Origin time	Latitude (°N.)	Longitude (°W.)	Z	Z*	M_D	M_W	gap	rms	*S-P*
1	93 530 1520 62.49	36 43.11	116 06.95	2.06	1.9	4.3	3.7	63	0.06	0.53
2	93 531 315 79.97	36 43.23	116 07.17	1.91	1.9	3.2	2.4	62	0.06	0.50
3	93 531 918 49.14	36 42.98	116 07.86	2.37	1.7	3.2	2.6	63	0.06	0.47
4	93 531 1113 67.99	36 43.41	116 06.66	1.86	1.0	2.7	2.1	61	0.06	0.48
5	93 531 1244 72.78	36 43.32	116 06.78	2.25	1.7	3.6	2.9	62	0.06	0.53
6	93 531 2238 47.40	36 43.32	116 07.09	1.84	1.7	2.7	2.0	61	0.09	0.57
7	93 6 1 1628 65.15	36 43.21	116 06.95	1.68	1.4	3.9	2.8	62	0.06	0.44
8	93 6 3 835 70.40	36 43.37	116 06.51	0.71	1.4	2.6	2.2	61	0.08	0.53
9	93 6 3 1720 32.89	36 42.96	116 07.49	1.80	1.7	3.3	2.4	63	0.07	0.47
10	93 6 4 1623 37.38	36 43.22	116 08.18	0.85	0.9	2.5	2.0	61	0.10	0.31
11	93 6 5 1323 71.33	36 42.89	116 07.67	1.63	1.1	3.4	2.5	70	0.06	0.39
12	93 6 6 1531 43.82	36 43.22	116 06.93	2.45	1.8	3.6	2.5	83	0.07	0.55

shows dominantly left lateral strike-slip motion on a northeast-striking high-angle structure (table 2). The first motion at near-source station RTPP provides good control on constraining the steeply dipping northeast-striking fault plane.

Earthquake Locations and Focal Mechanisms

Figure 4*A* shows the relocated epicenters of all earthquakes that triggered the regional network in 1993, and figure 4*B* is an expanded view showing the locations of the larger events and their focal mechanisms. Station RTPP is within about 1 km (epicentral distance) of most of the activity. Although locations of the smaller aftershocks exhibit some scatter, particularly at the south end of the sequence, all M 2+ events (generally higher quality locations) align along a narrow, northeast-striking, 200-m-wide trend. Table 1 is a detailed summary of earthquakes shown in figure 4*B*, and table 2 summarizes the first-motion focal mechanisms.

Table 2. Focal mechanisms.

[EV#, reference to figure 4*B* and table 1; strike, dip, and rake angles of northeast-striking fault plane (Aki and Richards, 1980; convention); focal mechanisms calculated with program FPFIT (Reasenberg and Oppenheimer, 1985]

EV#	Strike	Dip	Rake
1	50	85	–10
2	70	80	–20
3	80	80	20
4	72	80	–15
5	50	85	–10
6	70	90	20
7	50	85	–10
9	237	80	10
12	70	90	20

Shields and others (1995) have determined that the moment-magnitudes (M_w) for these shallow earthquakes are from 0.5 to 1.0 magnitude units lower than the SGBSN duration magnitudes (M_D). Such differences have not been observed between M_L and M_D for the LSM sequence (D.H. von Seggern, Univ. of Nevada-Reno, oral commun., 1993), and this difference may be the result of greater scattering of seismic energy for near-surface sources. The presence of a local cover of volcanic tuffs, for example, may lead to coda extension. A thorough assessment of the magnitude relationships for the Rock Valley sequence is not part of this study.

P-wave first-motion focal mechanisms for 10 of the largest earthquakes that triggered the portable instruments are shown in figure 4*B* and summarized in table 2. All mechanisms show predominantly left lateral strike-slip faulting on northeast-striking high-angle structures.

Evidence for Shallow Source Depths

The most convincing demonstration of the shallow depth of these earthquakes is from on-scale recordings of horizontal-component *S*-waves at portable station RTPP. Figure 5 shows two examples of the three-component waveforms for two events recorded at this station that exhibit very short *S* minus *P* times. In figure 5, the upper trace of each event is the vertical component and lower traces are the horizontal records for each event. The larger events of the sequence do not show larger *S* minus *P* times—which would imply greater depths. The event in figure 5*A* (reported in the SGBSN catalog as M 2.5) is one of the larger events from the sequence recorded at station RTPP. The *S* minus *P* time for this event at RTPP is about 0.3 seconds. The *S* minus *P* times for the first 250 events recorded at this station are

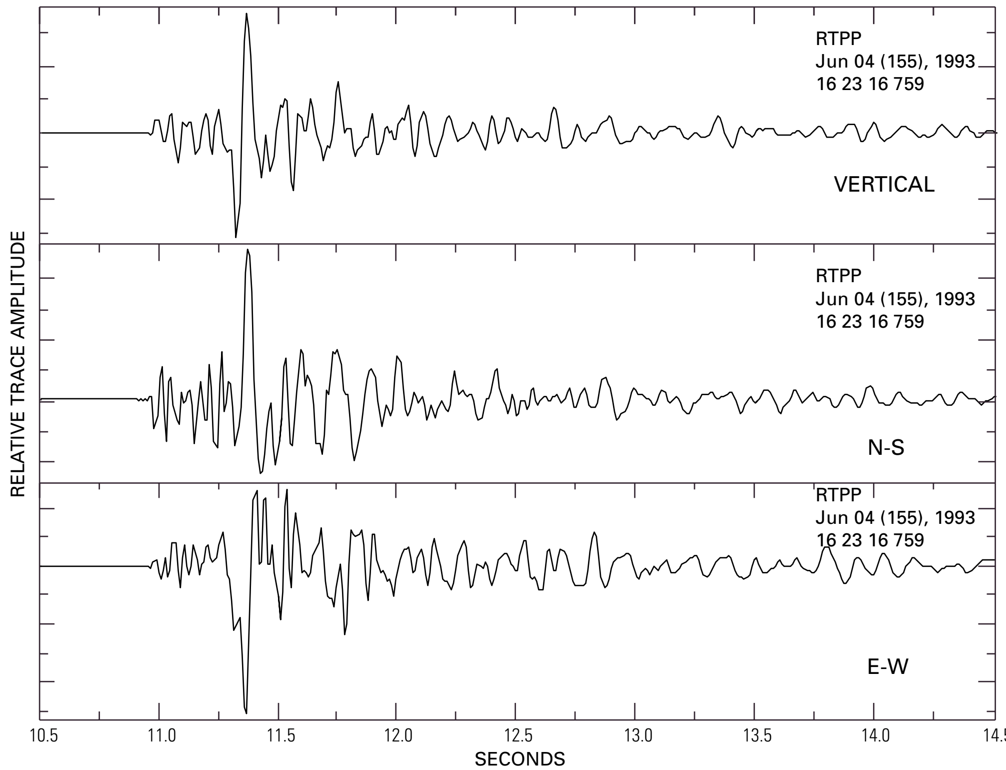

A

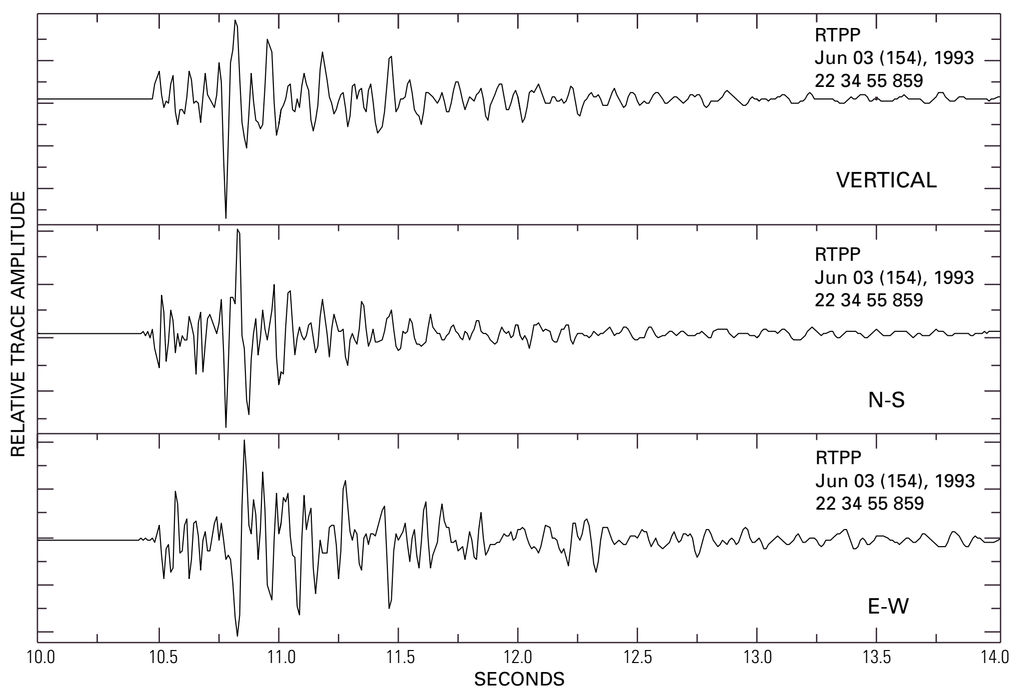

B

Figure 5. Examples of two events with unusually small *S* minus *P* times from the 1993 Rock Valley sequence recorded at station RTPP. Amplitudes are scaled to maximum trace amplitude per component to illustrate *S*-wave arrivals; peak amplitude of the three component recording for event *B* is about a factor of five less than that of event *A*.

shown in figure 6 (average ≈0.55 s). In figure 5, the hypocentral distance estimates from station RTPP are associated with selected *S* minus *P* times, an assumed *P*- to *S*-wave velocity ratio of 1.73, and a 3.0 km/s *P*-wave velocity (Hoffman and Mooney, 1984). Depths for an *S* minus *P* time of 0.5 s are also shown for 4.0 and 5.0 km/s *P*-wave velocities, respectively. Also shown in table 1 are the *S* minus *P* times observed for the events in figure 4*B*. The hypocentral depths for these earthquakes have been estimated from the epicenters using the relocation procedure and including the distance estimate to station RTPP from the *S* minus *P* time and 3 km/s upper layer *P*-wave velocity (table 1). Rodriguez and Yount (1988) have determined a *P*-wave velocity of 2.45 km/s for the upper surface layer of Tertiary sediments in the RVFZ using shallow seismic refraction techniques. Local velocities may vary significantly from these values. Because we have no direct estimates of the seismic velocities at depths from 3 to 5 km at this location in the RVFZ, we consider the hypocentral distances shown in figure 6 as maximum depth estimates.

Recent Earthquake Activity in Rock Valley

Between the time of 1992 LSM earthquake and August 1996, four M 3.5+ earthquakes have been recorded in the RVFZ (fig. 3). A March 1994 event was also measured at M_L 3.7 and was located at a depth of approximately 2 km adjacent to the Specter Range (fig. 3) near the southern boundary of the NTS (event location: lat 36°40.63′ N., long 116°13.28′ W.; SGBSN catalog location). In contrast to the 1993 sequence, however, this earthquake had essentially no aftershock activity. Portable instruments deployed immediately following March 1994 event recorded only one earthquake greater than M 2 and very few smaller events. The portable data confirmed that these earthquakes also occurred at shallow depth. The focal mechanism for the 1994 event is similar to those of the 1993 sequence, although it is less well constrained. The most recent M 3.5+ event occurred in the Specter Range at the south end of the fault segment or strand that apparently included the 1993 sequence (J.C. Yount, oral commun., 1995). This earthquake was located at 4.5 km depth and is clearly located in the Specter Range. The event triggered a recently installed strong-motion instrument (epicentral distance 4 km) and was followed by several M 2+ aftershocks; this was also a strike-slip event.

During the 1992 LSM aftershock sequence there was some activity in the RVFZ. Whether these earthquakes should be considered aftershocks of the LSM earthquake, or triggered activity on adjacent faults in the RVFZ, is a matter of definition. The largest of these were two M 3.5 events that locate at depth below the March 1994 M_L 3.7 event discussed in the preceding paragraph (fig. 3). In contrast to the March 1994 earthquake, these events occurred at 10 km depth, and a focal mechanism for one of the earthquakes exhibits a T-axis orientation more consistent with those observed for the LSM earthquake sequence (NW. orientation; fig. 3). This event also shows left-lateral strike-slip motion on a northeast-striking high-angle structure, and one of the fault planes aligns more closely with the general east-northeast trend of the RVFZ. The depth of this event is within the depth distribution (6–12 km) of the LSM sequence, whereas the more recent M 3.5+ events in this section of the RVFZ have been at shallower depths.

Another cluster of earthquake activity in the Spotted Range, east of the NTS (fig. 3), began in April of 1993 and continued for several weeks. These earthquakes occurred directly under SGBSN short-period station SPRG. *S* minus *P* times for this group of earthquakes are also on the order of 0.5 s, but the lack of a horizontal-component seismometer at this site makes it difficult to isolate *S*-wave arrivals and therefore to confirm the hypocentral depths. This activity is clearly south of the north-easterly trend of the RVFZ that is mapped along the Specter Range farther to the west. Several M 3+ earthquakes were recorded within this cluster of activity.

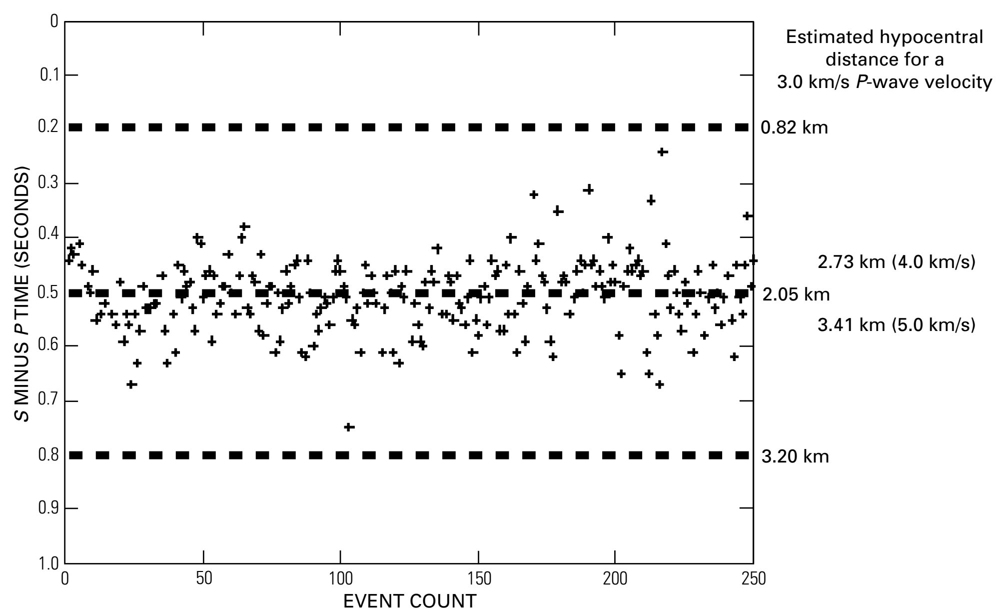

Figure 6. *S* minus *P* times for first 250 events recorded at portable station RTPP.

Summary and Conclusions

Tectonic earthquakes are rarely observed at depths of less than 3 km. Sanders (1990) suggested that in southern California very shallow earthquakes are confined to relatively stable blocks between major fault zones, and that the major fault zones themselves do not usually include shallow events. The wide range in the depth distribution of earthquakes in a published catalog spanning a broad region has usually been attributed to a lack of near-source station control or to generalized regional velocity models. Harmsen (1991) has reported small-magnitude shallow earthquake activity in the southern Great Basin at a number of locations including the RVFZ. Reported hypocentral depths may be called into question because of limited seismic station coverage in some areas in the southern Great Basin. Hypocentral constraints for earthquakes in the 1993 Rock Valley sequence were improved not only by data from the portable instruments but also by the addition of six short-period stations to the seismic network near Rock Valley following the 1992 LSM earthquake. Near-source recordings of the Rock Valley earthquakes constrain the depths of these events to less than 3 km. We have seen no evidence to date for mid-crustal depth (5–10 km) earthquake activity in this specific source area.

Rogers and others (1987) have discussed an apparent bimodal depth distribution of earthquake activity within the SGBSN, with a hiatus at approximately 4 km. A consideration of only the depths of earthquake activity since the 1992 LSM earthquake in the southern NTS also reveals a bimodal distribution. The LSM earthquake and its aftershock sequence were confined to between 6 and 12 km depth. In contrast, the 1993 M_L 3.7 Rock Valley earthquake, its associated aftershocks, and the 1994 Rock Valley earthquake occurred at shallow depths, leaving a gap in the hypocentral depth distribution between about 3 and 6 km depth. Because of fundamental difficulties in resolving earthquake depths (Gomberg, 1991), a determination as to whether this gap is characteristic of the entire southern Great Basin would require more sophisticated earthquake location techniques or the installation of near-source three-component instruments in the more active areas.

Recent shallow earthquake activity in the RVFZ (1993 and 1994) may be associated with near-surface tear faults or riedel shear structures above a throughgoing left-lateral shear zone, hence may not be reacting directly to the orientation of the prevailing tectonic stress field at depth. This is evidenced by the depth variation in Rock Valley focal mechanisms, although the data set is limited for deeper earthquakes. The local stress field and the geometry of buried fault planes determined from earthquake activity since 1992 (specifically LSM aftershocks) indicate a complex deformation pattern that is expressed on secondary structures in and around the RVFZ (Smith and others, this volume). The general north-south orientation of the P-axis for the focal mechanisms of the 1993 earthquakes indicates a component of north-south compression. A physical limitation in generating shallow earthquakes is that the lithostatic stress, as well as the frictional stress, must be high enough to initiate stick-slip faulting behavior. We speculate that the stress field imposed by the LSM earthquake could have contributed to an increase in shallow north-south-oriented compressional stresses. Also, shallow earthquake activity reported by Rogers and others (1987) may be localized to regions where relatively higher compressional stresses exist at shallow depths.

The distribution in the extension direction (T-axis) for the LSM sequence determined from more than 500 aftershock focal mechanisms trends N. 62° W. (Smith, Brune, and others, this volume) in contrast to the more east-west orientation of the T-axis for many of the Rock Valley focal mechanisms. This also implies a strike direction (northeast) for the predominantly normal faulting events of the LSM sequence that trends subparallel to the orientation of the high-angle northeast-striking strike-slip faulting earthquakes of the Rock Valley sequence. In other words, the analysis of the focal mechanisms of these two sequences suggests a difference in the local stress field between the LSM aftershock zone, 12 km to the west and at 6 to 10 km depth, and the segment of the RVFZ that generated the 1993 sequence. Whether this observed difference only reflects the shallow stress field in Rock Valley is a question that requires further studies of the focal mechanisms of earthquakes in the RVFZ.

The surface projection of the fault plane responsible for the 1992 LSM earthquake crops out in Jackass Flat (fig. 3), and faulting during this earthquake was predominantly dip slip (Meremonte and others, 1995; Harmsen, 1994, Smith and others, this volume). The fault plane strikes subparallel to the trend of the RVFZ, which, in contrast, has experienced dominantly strike slip displacement (Carr, 1990; O'Leary, this volume). These geometric relationships may be indicative of a style of deformation where displacement is partitioned between strike-slip and dip-slip faults (Wesnousky and Jones, 1994; Hardyman and Oldow, 1991), but this has previously been proposed in regions of much higher strain rates. From the analysis of earthquake focal mechanisms in and around the RVFZ during the past 2 years, it is clear that a variety of fault-plane and slip-vector orientations are present.

The Rock Valley sequence provides an important data set for understanding the seismic hazard from shallow earthquakes. For these earthquakes, near-source ground motion is dominantly a function of the local site effects and the properties of the earthquake source rather than path effects (attenuation and geometrical spreading). Moderate-sized shallow earthquakes may generate ground motions critical to the design of engineered facilities. Whether shallow earthquakes such as those observed in the RVFZ are capable of occurring on faults near Yucca Mountain may be a function of the local style of deformation. Very little strike-slip motion has been observed from trenching studies on the faults at Yucca Mountain (Menges and others, 1994), whereas the RVFZ is a zone of distributed strike-slip deformation that is related to other northeast-striking faults in the central NTS.

There is strong evidence that the June 29, 1992, LSM earthquake was triggered by the June 28, 1992, M 7.4 Landers, Calif., earthquake (Hill and others, 1993; Anderson and others, 1994; Smith, Brune, and others, this volume). The observed increase in seismicity in the RVFZ may also have been triggered by the Landers earthquake, either directly, as evidence suggests for the LSM earthquake, or indirectly, through effects of the LSM event itself. It is also possible that a slow creep event may have been initiated in the deep crust in the Rock Valley area by the Landers event, which, in turn, has been expressed as an increase in the local seismicity.

Because of the unusual nature of earthquakes in the RVFZ, we believe that continued analysis of these events may lead to important insights into earthquake source mechanisms, a better understanding of the tectonics of the southern NTS, and more precise estimates of the seismic hazard from shallow earthquake activity in the region.

References Cited

Aki, K., and Richards, P., 1980, Quantitative seismology—Theory and methods: San Francisco, W.H. Freeman.

Anderson, J.G., Brune, J.N., Louie, J.N., Zeng, Y., Savage, M., Yu, G., Chen, Q., and dePolo, Diane, 1994, Seismicity in the western Great Basin apparently triggered by the Landers, California, earthquake, 28 June 1992: Bulletin of the Seismological Society of America, v. 84, p. 863–891.

Carr, W.J., 1984, Regional structural setting of Yucca Mountain, Southwestern Nevada, and late Cenozoic rates of tectonic activity in part of the southwestern Great Basin, Nevada and California: U.S. Geological Survey Open-File Report 84-854.

———1990, Styles of extension in the Nevada Test Site region, southern Walker Lane Belt—An integration of volcano-tectonic and detachment fault models, *in* Wernicke, B.P., ed., Basin and Range extensional tectonics near the latitude of Las Vegas, Nevada: Geological Society of America Memoir 176, p. 283–303.

Fletcher, J., Harr, L., Hanks, T., and Baker L., 1987, The digital array at Anza, California; processing and initial interpretation of source parameters: Journal of Geophysical Research, v. 92, p. 369–382.

Frankel, A., Fletcher, J., Vernon, F., Harr, L., Berger, J., Hanks, T., and Brune, J.N., 1986, Rupture characteristics and tomographic source imaging of $M_L \approx 3$ earthquakes near Anza, southern California: Journal of Geophysical Research, v. 91, p. 12633–12650.

Gomberg, Joan, 1990, The effect of *S*-wave arrival times on the accuracy of hypocentral estimation: Bulletin of the Seismological Society of America, v. 80, p. 1580–1604.

———1991, Seismicity and detection/location threshold in the Southern Great Basin Seismic Network: Journal of Geophysical Research, v. 96, p. 16401–16414.

Hamilton, R.M., Smith, B.E., Fisher, F.G., and Papnek, P.J., 1971, Seismicity of the Pahute Mesa area, Nevada Test Site, 8 December 1968 through 31 December 1970: U.S. Geological Survey Special Studies-89 474-138.

Hardyman, R.F., and Oldow, J.S., 1991, Tertiary tectonic framework and Cenozoic history of the central Walker Lane, Nevada, *in* Raines, G.L., Lisle, R.E., Schafer, R.W., and Wilkinson, W.H., eds., Geology and ore deposits of the Great Basin: Geological Society of Nevada, Symposium Proceedings, Reno, Nevada, p. 279–301.

Harmsen, S.C., 1994, The Little Skull Mountain, Nevada, earthquake of June 29, 1992—Aftershock focal mechanisms and tectonic stress field implications: Bulletin of the Seismological Society of America, v. 84, p.1484–1505.

———1991, Seismicity and focal mechanisms for the Southern Great Basin of Nevada and California in 1991: U.S. Geological Survey Open-File Report 92-340.

Hill, D.P., Reasenberg, R.A., Michael, A., Arabaz, W.J., Beroza, G., Brumbaugh, D., Brune, J.N., Castro, R., Davis, S., dePolo, Diane, Ellsworth, W.L., Gomberg, Joan, Harmsen, S.C., House, L., Jackson, S.M., Johnston, M.J.S., Jones, L., Keller, R., Malone, S., Munguia, L., Nava, S., Pechmann, S.J., Sanford, A., Simpson, R.W., Smith, R.B., Stark, J., Stickney, M., Vidal, A., Walter, S., Wong V., and Zollweg, J., 1993, Seismicity remotely triggered by the magnitude 7.3 Landers, California, earthquake: Science, v. 260, p. 1617–1623.

Hoffman, L.R., and Mooney, W.D., 1984, A seismic study of Yucca Mountain and vicinity, southern Nevada—Data report and preliminary results: U.S. Geological Survey Open-File Report 83-588, 50 p.

Menges, C.M., Wesling, J.R., Whitney, J.W., Swan, F.H., Coe, J.A., Oswald, J.A., and Thomas, A.P., 1994, Preliminary results of paleoseismic investigations of Quaternary faults on eastern Yucca Mountain, Nye County, Nevada, *in* High-Level Radioactive Waste Management: Proceedings of the Fifth International Conference, Las Vegas, Nev., May, 1994, American Nuclear Society, LaGrange Park, Ill., v. 4, p. 2373–2390.

Meremonte, M.E., Gomberg, Joan, and Cranswick, Edward, 1995, Constraints on the 29 June 1992 Little Skull Mountain sequence provided by robust hypocentral estimates: Bulletin of the Seismological Society of America, v. 85, p. 1039–1049.

Peppin, W.A., and Nicks, W.F., 1992, Real time analog and digital data acquisition through CUSP: Seismological Research Letters, v. 63, p. 181–189.

Reasenberg, P.A. and Oppenheimer, D., 1985, FPFIT, FPPLOT, and FPPAGE; Fortran computer programs for calculating and displaying earthquake fault-plane solutions: U.S. Geological Survey Open-File Report 85-739.

Rodriguez, E.A., and Yount, J.C., 1988, Relation between *P*-wave velocity and stratigraphy of late Cenozoic deposits of southern Nevada, *in* Carr, M.D. and Yount, J.C., eds.,Geologic and hydrologic investigations of a potential nuclear waste disposal site at Yucca Mountain, southern Nevada: U.S. Geological Survey Bulletin 1790, p. 139–146.

Rogers, A.M., Harmsen, S.C., and Meremonte, M.E., 1987, Evaluation of the seismicity of the southern Great Basin and its relationship to the tectonic framework of the region: U.S. Geological Survey Open-File Report 87-408.

Rogers, A.M., Harmsen, S.C., Corbett, E.J., Priestly, K.F., and dePolo, Diane, 1991, The seismicity of Nevada and some adjacent parts of the Great Basin, *in* Slemmons, D. B., Engdahl, E. R., Zoback, M.D., and Blackwell, D.D., eds., Neotectonics of North America: Geological Society of America, Decade of North American Geology, Map Volume 1, p. 153–184.

Sanders, C.O., 1990, Earthquake depths and the relation to strain accumulation and stress near strike-slip faults in southern California: Journal of Geophysical Research, v. 95, p. 4751–4762.

Savage, M.K., and Anderson, J.G., 1995, A local magnitude scale for the western Great Basin-eastern Sierra Nevada from synthetic Wood-Anderson seismograms: Bulletin of the Seismological Society of America, v. 85, p. 1236–1245.

Shields, G., Smith, K.D. and Brune, J.N., 1995, Source parameters of a sequence of very shallow earthquakes in the Rock Valley fault zone, southern Nevada Test Site [abs.]: Eos, v. 76, p. F426.

Wesnousky, S., and Jones, C., 1994, Oblique slip, slip partitioning, spatial and temporal changes in the regional stress field, and the relative strength of active faults in the Basin and Range, western United States: Geology, v. 22, p. 1031, 1034.